6.3 Evaluation of CCMs

6.3.1 Evaluation of Photolysis Rates

The accurate calculation of photolysis (J) rates is an essential component of any atmospheric chemical model. However, this calculation is complicated and there is a lot of potential for differences between models. Models may differ in their treatment of radiative transfer, aerosols and clouds. Models may update the photolysis rates at a different time resolution. Although all models may use standard absorption cross sections (e.g. JPL 2006), they may differ in how they parameterise temperature dependencies etc.

For these reasons it is important to intercompare photolysis rates calculated by CCMs. For a critical comparison these rates need to be intercompared using prescribed conditions (e.g. O_3, T, p profiles) but using the code actually used in the CCM. Also, it is important to compare the overall modelled J rates. This comparison combines testing the modelled radiative transfer and the assumed cross sections. Although this factors in more terms, it compares the quantity actually relevant for the chemical comparisons.

6.3.1.1 Introduction

This photolysis benchmark (PhotoComp-2008, or PC'08) is a component of the SPARC CCMVal Chapter 6 and, has been designed to evaluate how models calculate photolysis rates (and indirectly heating rates) in the stratosphere and troposphere. The primary goal is to improve model performance due to better calibration against laboratory and atmospheric measurements and to more accurate numerical algorithms for solving the equation of radiative transfer. As with specific subsections of any major model comparison (e.g., Prather and Remsberg, 1993), there are numerous mistakes due to a different interpretation of the experiment, there are simple mistakes in model coding, there are different sources of physical data (solar fluxes, cross sections, quantum yields), and there are many different approximations of the exact solution. Any of these can make a model an "outlier" for one particular test, and thus the analysis must strive to identify these outliers as quickly as possible and provide clues as to the cause. This does not always mean that the majority rules, but in most cases, a singularly unusual J-value profile for a model is in error.

For this comparison, we do not establish a single model as a reference (but not necessarily correct) standard, but instead define a robust mean and standard deviation from the ensemble of contributing models (see **Table 6-1**). The J-values are converted to ln(J) and averaged. A lower altitude cutoff is made where $J < 10^{-10}$ /sec (or 10^{-14} /sec for J-O2). Models that fall more than 2 standard deviations (in ln(J)) from the mean over the middle of this altitude range are eliminated from the ensemble and an new "robust"

mean and standard deviation are computed. This method quickly identified outliers with obvious mistakes (e.g., an incorrect O_3 profile was specified in the LMDZ results reported here).

6.3.1.2 PhotoComp-2008 Experiments

There arre 3 parts to the photolysis intercomparison which are summarized below. Full details are available online (http://homepages.see.leeds.ac.uk/~lecmc/ccmvalj , linked from CCMVal pages):

Part 1is a basic test of all J-values for high sun (SZA = 15º) over the ocean (albedo = 0.10, Lambertian). **Part 1a**: Clear sky (only Rayleigh scattering) and no aerosols. **Part 1b**: Pinatubo aerosol in the stratosphere (layer 10). **Part 1c**: Stratus cloud (layer 2). The primary atmosphere was specified in terms of pressure layers, mean temperature, and column O_3 in each layer. Absorption by NO_2 or other species was not included in calculating optical depths.

Part 2 tests the simulation of a spherical atmosphere and twilight conditions that are critical to the polar regions. It used the same atmosphere as Part 1 without clouds or aerosols and assumed equinox (solar declination = 0º) and a latitude of 84ºN. The surface SZA (not including refraction) therefore varies from 84º (noon) to 96º (midnight). J values were reported at noon, midnight, and the 24-hour average (integrating as done in the CCM).

Part 3 tests the accuracy of wavelength binning in the critical region 290-400 nm that dominates tropospheric photolysis. Rayleigh scattering and surface reflection were switched off (albedo = 0) giving effectively a simple Beer's Law calculation. The calculation repeated Part 1, but report only J-values for J-O3 (i.e., total), J-O3(1d) [O3 => O2 + O(1D)], and J-NO2 [NO2 => NO + O]. These are the two critical J-values for the troposphere, and they both have unusual structures in absorption cross section and quantum yields. Reference runs were done using very high resolution (0.05 nm) cross sections and solar fluxes and for different options (e.g., JPL-06 vs. IUPAC cross sections) to provide a benchmark. Results for Part 3 focus below 24 km.

A standard atmosphere, whose primary definition is in terms of the air mass (pressure thickness), ozone mass, and mean temperature in each layer was specified. This chosen atmosphere is typical of the tropics with total ozone column of 260 DU. The use of JPL-2006 data (same as main CCM runs) was encouraged. High-resolution solar fluxes as a reference (sun-earth distance = 1.0 au, averaged over the 11-yr solar cycle) were also provided.

Table 6-1 Models contributing to PhotoComp-2008

Group	Model	P1a	P1 b	P1 c	P2-24hr	P2-noon	P2-midn	P3	Doc	Participants
GFDL, USA	AMTRAC	√			√	√	√			John Austin
NIES, Japan	CCSRNIES	√	√		√	√	√		√	Hideharu Akiyoshi
MPIC, Mainz Germany	EMAC	√		√	√	√			√	R. Sander C. Bruehl
GSFC, USA	FastJX	√	√	√	√	√	√	√	√	Huisheng Bian
GSFC, USA	(??)	√			√	√	√			Randy Kawa Richard S. Stolarski
LMDZrepro	TUV4.1	√	√	√	√	√	√	√		Sandrine Lefebvre Slimane Bekki
Niwa	SOCOL v2.0	√		√	√	√			√	Dan Smale Tatiana Egorova Eugene Rozanov
NCAR, USA	TUV	√	√	√	√	√	√	√	√	Sasha Madronich
UCI	FastJX	√	√	√	√	√	√	√	√	Michael Prather
Univ. Leeds, UK	UMSLIMCAT	√			√	√	√			Martyn Chipperfield Miriam Sinnhuber
	UNM									
NCAR, USA	WACCM	√			√	√	√	√		Doug Kinnison

6.3.1.3 PhotoComp-2008 Results and Discussion

This brief summary here presents a preliminary analysis and we expect that as the participants look in more detail for certain J-values, we will be able to identify the cause of some of these larger discrepancies and perhaps relate it to current scientific uncertainty, or at least to tow different scientific choices on methods or data. More plots will be provided online (see above web link).

Figure 6-1 shows the deviations in ln(J) for 9 different J-values from experiment P1a. The agreement among the core models (those within 2 std dev) is really excellent for many J-values. Some models consistently fall outside this core and it appears to be due to the method of solving the radiative transfer equation (e.g., look-up tables) or to mistakes in implementing the experiment (e.g., LMDZ's wrong O3 profile). The spread in J-NO is not too bad (±20% above 1 hPa), but it appears to be bi-modal and may reflect the failure of some models (e.g., UCI) to account for NO self-absorption above the mesopause. In other cases the core range is very small (e.g., for N2O and CFCl3) but much larger for CF2Cl2 (see **Figure 6-1** as well as summary tables of robust standard deviations in **Table 6-2**). This can only be explained by differences in the cross sections for CF2Cl2. Other oddities stand out, e.g., the very large ±30% range in J-H2COa, which probably reflects the different partitioning of photolysis products (vs. J-H2COb).

Figure 6-2 has four sections. The first shows the robust mean $\log_{10}$(J) for NO, O2 and O3 for experiments P1a and P2 (n, a, m). The second shows the deviations from the mean for the 24-hour average rates P2a. In this case the J-NO has expectedly large ranges, but the core models show a very small std dev for J-O2 and J-O3. The latter is particularly important for heating rates at the pole. The last two sections show the change in J-values for a Pinatubo-like aerosol layer (P1b) and a thick stratus cloud (P1c). Far fewer models were able to do these experiments, and in general the agreement is reasonable, showing enhancements above and within the scattering layer and reductions at the surface.

Figure 6-3 shows a blow-up of the five models (GSFC, LMDZ, TUV, UCI, WACCM) that submitted thirteen different results for experiment P3. A few models integrated J-NO2 with extremely high wavelength resolution (e.g., 0.05 nm) and other versions of the same model used very coarse wavelength bins (e.g., fast-JX). Other differences include how the temperature effects were interpolated or extrapolated. Overall, these differences in experiment P3 were small: standard deviations (without LMDZ) were 0.8 to 1.6% for J-NO2, 0.9 to 1.7% for J-O3(1D), and 1.0 to 2.0% for J-O3(total).

Table 6-2 summarizes the robust std dev for the altitudes of interest (see table text). For many J-values we find exceedingly good agreement, for example the calculation of J-O3(total) has a std dev of only 4%. Similar agreement is found for H_2O_2, NO_2, HNO_2, HOCl, BrO, N_2O, $CFCl_3$, halon-1301; but there is surprisingly large std dev for CF_2Cl_2 (noted above), H2COa/b, ClNO3a/b, HNO_4 (*near-IR photolysis not included?*), J-O3 is a

key heating rate term, and the ability to calculate this to within 4% from SZA=15 to 84 degrees is excellent (*though CCM photolysis schemes are NOT necessarily linked to heating rate calculations*..). The average J-O3 (SZA from 84 to 96), however is twice as uncertain, and the twilight values for most of the J-values (P2m) have much larger std dev.

Table 6-2. Robust Standard Deviation (RSD) of ln(J) x 100 (%) is derived by (1) calculate the mean ln(J) from all contributing models; (2) drop all lower levels where the average J is < 1.e-10 (or <1.e-14 for J-O2); (3) drop any model outside of 2 std dev for levels ranging from 3 above the lowest level in step 2 up to 3 below the top level (~80 km); recalculate this robust mean ln(J) and robust std dev (RSD) for the remaining models. Models that fail the 2-std-dev test are labelled in the figure legend with an asterisk (*); and those that did not report that particular J-value, with an ampersand (&). The std dev below is the average of the robust std dev for levels from 4 above the lowest in step 2 to 4 below the top (~72 km). Results are shown for experiments P1a (SZA=15) and P2 for noon (n, SZA=84), for 24-hr average (a), and for midnight (m, SZA=96).

no.	J-value	P1a	P2n	P2a	P2m	no.	J-value	P1a	P2n	P2a	P2m
1	J-NO	19.	30.	34.	0.	31	J-F115	28.	35.	43.	0.
2	J-O2	8.	10.	11.	0.	32	J-CCl4	5.	10.	10.	0.
3	J-O3	4.	4.	9.	29.	33	J-CH3Cl	7.	6.	11.	0.
4	J-O3(1D)	8.	11.	11.	80.	34	J-MeCCl3	8.	7.	13.	0.
5	J-H2COa	27.	45.	23.	29.	35	J-CH2Cl2	0.	0.	5.	0.
6	J-H2COb	18.	19.	33.	25.	36	J-CHF2Cl	20.	22.	26.	0.
7	J-H2O2	5.	7.	11.	20.	37	J-F123	15.	8.	9.	0.
8	J-CH3OOH	6.	8.	15.	19.	38	J-F141b	8.	5.	11.	0.
9	J-NO2	3.	6.	11.	15.	39	J-F142b	24.	11.	11.	0.
10	J-NO3	8.	9.	14.	31.	40	J-CH3Br	5.	9.	11.	0.
11	J-N2O5	11.	12.	16.	23.	41	J-H1211	6.	4.	13.	489.
12	J-HNO2	3.	4.	4.	11.	42	J-H1301	4.	4.	5.	0.
13	J-HNO3	7.	8.	17.	83.	43	J-H2402	1.	1.	9.	0.
14	J-HNO4	15.	50.	67.	240.	44	J-CH2Br2	23.	21.	25.	0.
15	J-ClNO3a	15.	15.	15.	24.	45	J-CHBr3	12.	21.	23.	252.
16	J-ClNO3b	7.	12.	14.	28.	46	J-CH3I	9.	8.	10.	14.
17	J-Cl2	7.	5.	16.	24.	47	J-CF3I	0.	2.	6.	8.
18	J-HOCl	5.	7.	13.	14.	48	J-OCS	13.	17.	27.	0.
19	J-OClO	8.	8.	13.	27.	49	J-PAN	6.	9.	16.	62.
20	J-Cl2O2	14.	13.	18.	30.	50	J-CH3NO3	4.	8.	12.	48.
21	J-ClO	11.	10.	13.	49.	51	J-ActAld	41.	45.	49.	47.
22	J-BrO	3.	12.	20.	13.	52	J-MeVK	5.	6.	7.	18.
23	J-BrNO3	6.	6.	10.	26.	53	J-MeAcr	10.	9.	9.	8.
24	J-HOBr	3.	5.	9.	24.	54	J-GlyAld	17.	20.	22.	50.
25	J-BrCl	7.	6.	11.	25.	55	J-MEKeto	11.	11.	11.	18.
26	J-N2O	3.	7.	14.	0.	56	J-EAld	11.	14.	16.	30.
27	J-CFCl3	3.	10.	10.	0.	57	J-MGlyxl	21.	25.	38.	51.
28	J-CF2Cl2	10.	12.	15.	0.	58	J-Glyxla	26.	46.	56.	126.
29	J-F113	6.	12.	13.	0.	59	J-Glyxlb	45.	50.	54.	86.
30	J-F114	9.	7.	13.	0.	60	J-Acet-a	12.	35.	36.	67.

6.6 Figures

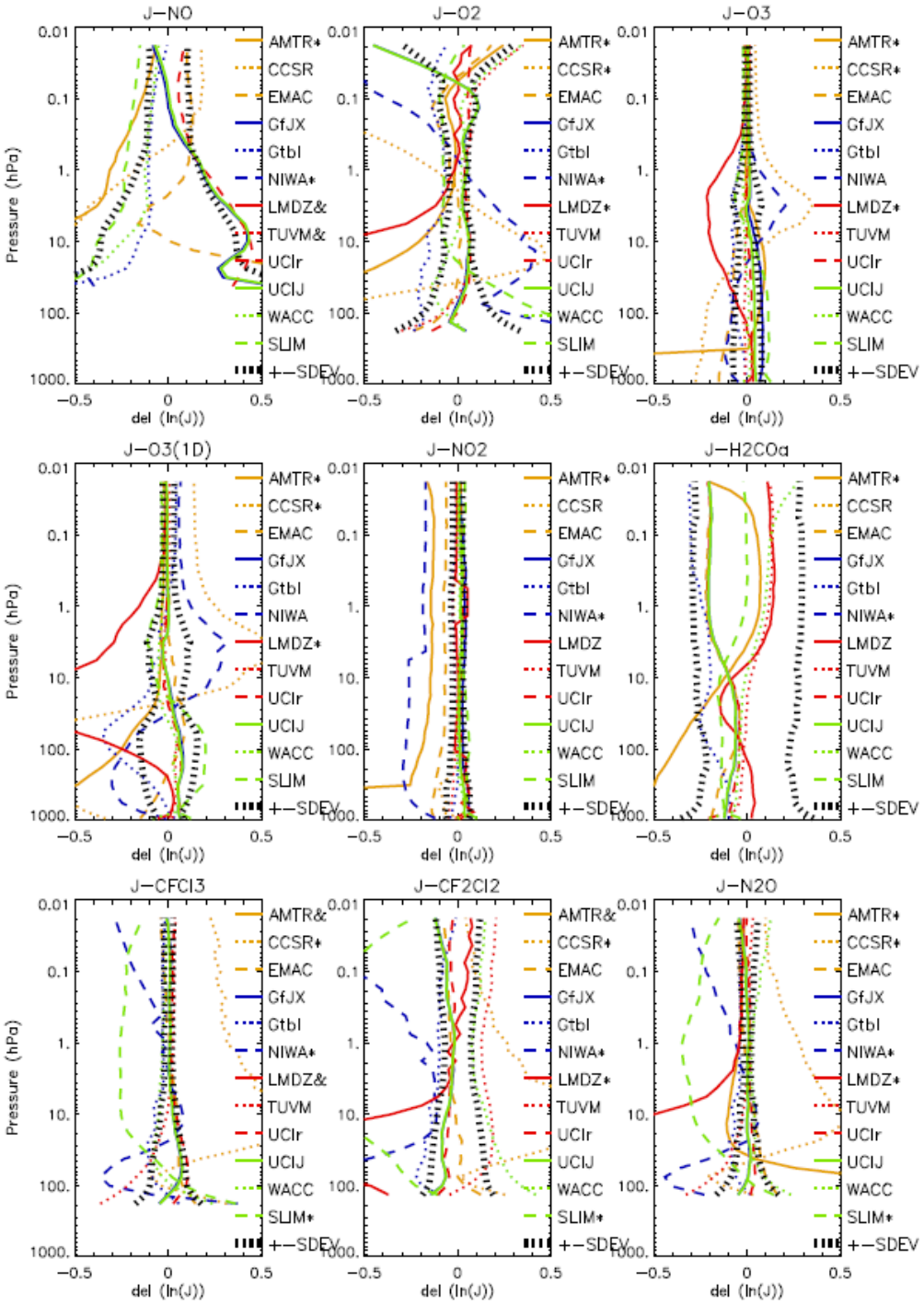

Figure 6-1. Model deviations from the robust mean ln(J) for some sample J-values as a function of altitude. The x-axis is in natural log units (approximately -50% to +50%). See **Table 6-2** for definition of the robust mean and std dev (shown as black hatched line) as well as the legend labels.

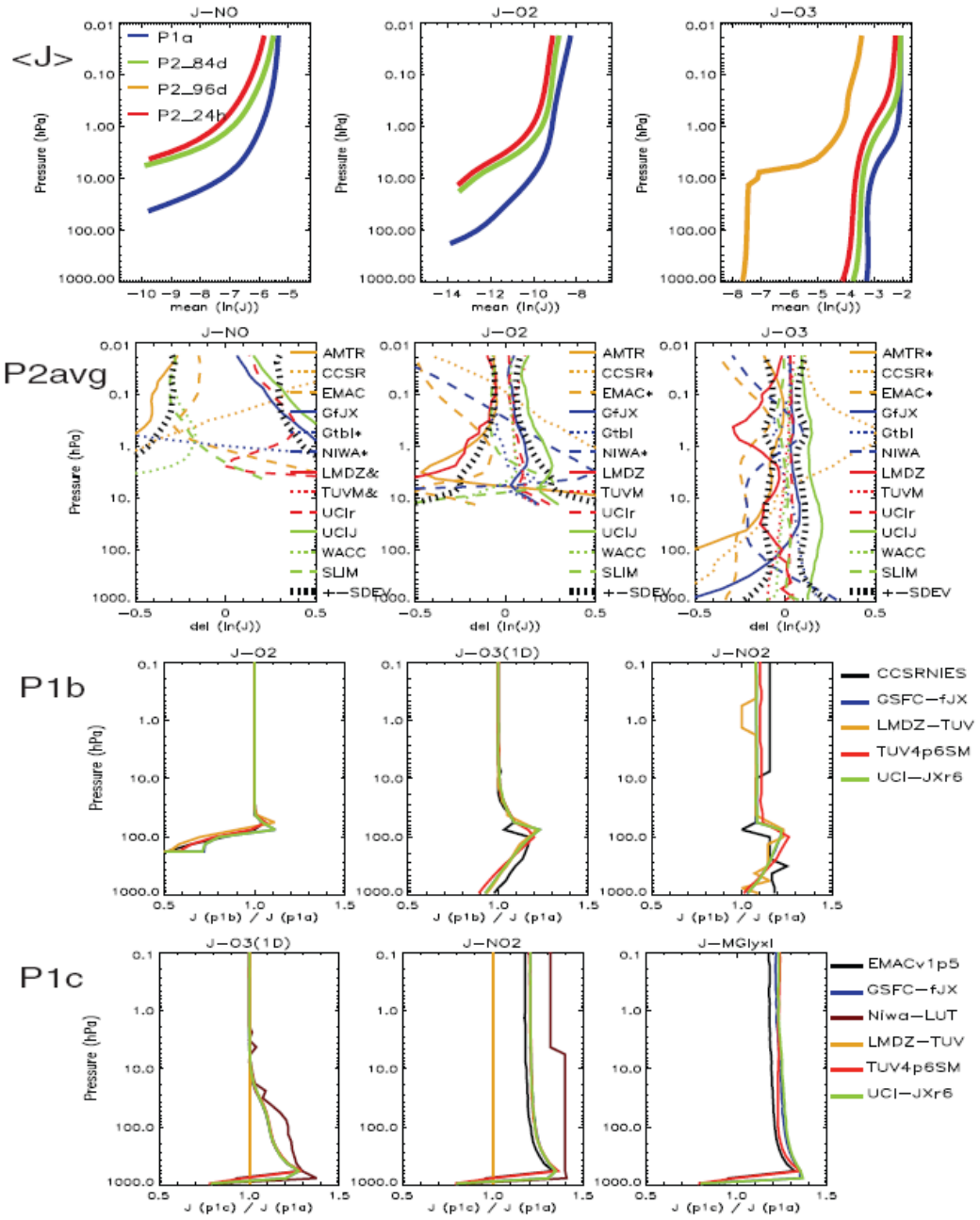

Figure 6-2. (a) Robust mean ln(J(/sec)) for NO, O_2, and O_3 shown for experiments P1a and P2 for noon (SZA=84), midnight (SZA=96) and 24-hr average. (b) As in **Figure 6-1**, the model deviations in ln(J) for the same three J-values are shown for experiment P2avg. (c) Change in J-values (O_2, O_3(1D), NO_2) for Pinatubo-like cloud in the lower stratosphere. The ratio P1b/P1a is plotted vs. altitude. The participating models are given in the legend. (d) Change in J-values (O3(1D), NO2, MethylGloxyl) for a thick stratus cloud. The ratio P1c/P1a is plotted vs. altitude. The participating models are given in the legend. The erratic jumps in this ratio for a few models is caused by the lack of precision (only 2 decimal places) in reporting.

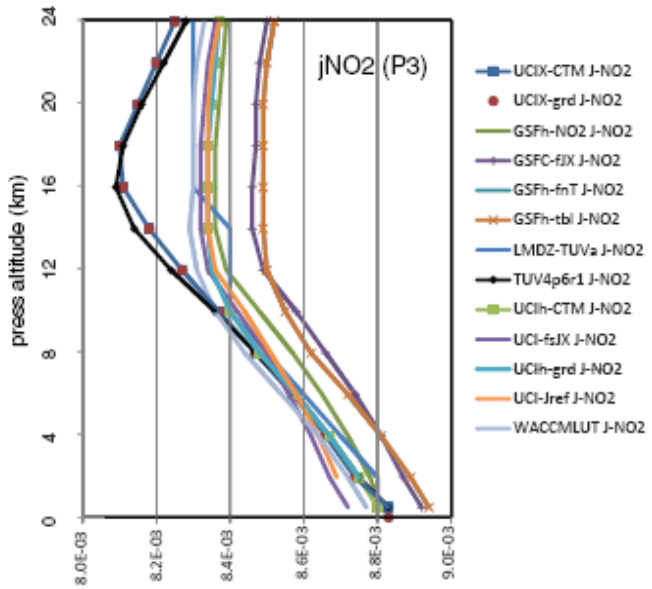

UCIX-CTM	0.05 nm (solar, O3), 1 nm (NO2); NO2 (Xs & q) log extrap to all T
UCIX-grd	0.05 nm (solar, O3), 1 nm (NO2); NO2 (Xs & q) log extrap to all T
GSFh-NO2	0.05 nm (solar, O3), 1 nm (NO2); O3 (Xs & q) = fn(T), NO2 (Xs & q) linear between 220 - 298K
GSFC-fJX	std fast-JX: bin mid-pts = 295-303-310-316-333-380-574 nm
GSFh-fnT	0.05 nm (solar, O3, NO2 interp); O3 (Xs & q) = fn(T), NO2 (Xs & q) log extrap to all T
GSFh-tbl	0.05 nm (solar, O3, NO2 interp); O3 (Xs & q) tables for 180K-260K-300K, NO2 (Xs & q) log extrap to all T
LMDZ-TUVa	- - -
TUV4p6SM	1 nm (208-430 nm), 2 nm out to 700 nm
UCIh-CTM	0.05 nm (solar, O3), 1 nm (NO2); NO2 (Xs & q) linear between 220 - 298K
UCI-fsJX	std fast-JX: bin mid-pts = 295-303-310-316-333-380-574 nm
UCIh-grd	0.05 nm (solar, O3), 1 nm (NO2); NO2 (Xs & q) linear between 220 - 298K
UCI-Jref	1 nm (295-320 nm), 2 nm (320-324), 10 nm (325-385nm),...
WACCMLUT	- - -

Figure 6-3. J-NO2 (/sec) from experiment P3 is shown for the troposphere and lower stratosphere. In this experiment (SZA=15, no scattering, no surface reflection, and only O_3 absorption) the primary differences are due to the absolute values of the NO_2 cross sections and quantum yields and to the method used to extrapolate to cold temperatures (12-20 km). The wavelength resolution has little impact (compare the sequence UCIh-CTM, UCI-Jref, UCI-fsJX). Overall this is a very small spread: ~1% std dev below 12 km.